



Geophysical Research Letters

RESEARCH LETTER

10.1002/2017GL075788

Key Points:

- Both moderate and intense MS waves were observed well off the geomagnetic equator
- Off-equatorial MS waves can cause the electron pitch angle scattering and momentum diffusion on timescales of a day
- Off-equatorial MS waves with intense amplitude can produce electron butterfly distributions at \sim 100 keV to $>$ 1 MeV within an hour

Supporting Information:

- Supporting Information S1

Correspondence to:

B. Ni,
bbni@whu.edu.cn

Citation:

Ni, B., Zou, Z., Fu, S., Cao, X., Gu, X., & Xiang, Z. (2018). Resonant scattering of radiation belt electrons by off-equatorial magnetosonic waves. *Geophysical Research Letters*, 45, 1228–1236. <https://doi.org/10.1002/2017GL075788>

Received 21 SEP 2017

Accepted 23 JAN 2018

Accepted article online 29 JAN 2018

Published online 10 FEB 2018

Resonant Scattering of Radiation Belt Electrons by Off-Equatorial Magnetosonic Waves

Binbin Ni¹ , Zhengyang Zou¹ , Song Fu¹ , Xing Cao¹ , Xudong Gu¹ , and Zheng Xiang¹

¹Department of Space Physics, School of Electronic Information, Wuhan University, Wuhan, China

Abstract Fast magnetosonic (MS) waves are commonly regarded as electromagnetic waves that are characteristically confined within $\pm 3^\circ$ of the geomagnetic equator. We report two typical off-equatorial MS events observed by Van Allen Probes, that is, the 8 May 2014 event that occurred at the geomagnetic latitudes of 7.5° – 9.2° both inside and outside the plasmasphere with the wave amplitude up to 590 pT and the 9 January 2014 event that occurred at the latitudes of $-(15.7^\circ$ – $17.5^\circ)$ outside the plasmasphere with a smaller amplitude about 81 pT. Detailed test particle simulations quantify the electron resonant scattering rates by the off-equatorial MS waves to find that they can cause the pitch angle scattering and momentum diffusion of radiation belt electrons with equatorial pitch angles $<$ $\sim 75^\circ$ or $<$ $\sim 58^\circ$ (depending on the wave latitudinal coverage) on timescales of a day. Subsequent two-dimensional Fokker-Planck diffusion simulations indicate that the strong off-equatorial MS waves are capable of efficiently transporting high pitch angle electrons to lower pitch angles to facilitate the formation of radiation belt electron butterfly distributions for a broad energy range from \sim 100 keV to $>$ 1 MeV within an hour. Our study clearly demonstrates that the presence of off-equatorial MS waves, in addition to equatorial MS waves, can contribute importantly to the dynamical variations of radiation belt electron fluxes and their pitch angle distribution.

1. Introduction

Fast mode magnetosonic (MS) emissions, also called “equatorial noise,” are linear polarized whistler mode electromagnetic waves with the frequencies ranging from the proton cyclotron frequency (f_{cp}) to lower hybrid resonance frequency (f_{LHR}) (e.g., Balikhin et al., 2015; Chen & Thorne, 2012; Russell et al., 1970; Santolík et al., 2002). Previous studies (e.g., Ma et al., 2013, 2016; Meredith et al., 2008; Tsurutani et al., 2014) have shown that MS emissions occur characteristically within 3° of the terrestrial geomagnetic equator at $L = 2$ – 8 both inside and outside the plasmasphere, along with the substantial decrease in the wave occurrence rate at higher latitudes. Triggered by the ring distribution of energetic protons, MS waves are initially excited with very oblique wave normal angles and then propagate in both radial and azimuthal directions that are nearly perpendicular to the background magnetic field (e.g., Chen et al., 2011; Xiao, Zhou, et al., 2015). Recent observations also reported that, besides the frequently present harmonic structures (e.g., Balikhin et al., 2015), MS waves occasionally consist of discrete wave elements with the rising tone (e.g., Boardsen et al., 2014; Fu et al., 2014) and “zipper-like” periodic structures (Li et al., 2017).

The importance of MS waves is well recognized since this kind of wave mode has been proposed as a viable acceleration candidate through Landau resonance to energize radiation belt electrons to approximate MeV energies on a timescale of \sim 1 day, comparable to that of chorus wave-induced electron acceleration (Horne et al., 2007). Transit time scattering by MS waves are also found to contribute to the radiation belt electron dynamics (Bortnik & Thorne, 2010; Li et al., 2014). Recent studies further stated that scattering by MS waves can provide an efficient mechanism for energetic electron diffusion in the slot region and outer radiation belt and primarily account for the formation of electron butterfly or top-hat distributions in the inner magnetosphere (Li, Ni, et al., 2016; Li, Bortnik, et al., 2016; Ni et al., 2017; Xiao, Yang, et al., 2015). In addition, Fu et al. (2016) found that MS waves can potentially accelerate ring current protons at a few keV inside the plasmasphere and at \sim 10 keV outside the plasmasphere.

It is worthwhile to point out that all the above quantitative analyses concentrated on the equatorial MS waves, that is, within $|\lambda| < \sim 3^\circ$. In contrast, off-equatorial MS waves receive much less attention, while these waves have been reported as well in the literature. Based on the Polar satellite data, Tsurutani et al. (2014) illustrated a number of small-amplitude MS wave events that occurred at the geomagnetic latitudes as

high as $+20^\circ$ and as low as -60° near the midnight sector in the plasmasphere. A following study of Zhima et al. (2015) reported a stronger off-equatorial MS wave event observed at $\lambda = -$ (16.5° to 17.9°) by Van Allen Probes and investigated their underlying source via ray tracing simulations. While it is currently recognized that both moderate and intense MS waves can be observed well off the geomagnetic equator, their effects of wave-particle interactions on the radiation belt electron dynamics remain unknown. The present study reports two representative off-equatorial MS events observed by the Van Allen Probes, specifically, the 8 May 2014 event that occurred at the magnetic latitudes of 7.5° to 9.2° both inside and outside the plasmasphere with the wave amplitude up to 590 pT, and the 9 January 2014 event that occurred at the latitudes of $-$ (15.7° to 17.5°) outside the plasmasphere with a lower amplitude, about 81 pT. Through test particle modeling and 2-D Fokker-Planck diffusion simulations, we find that strong off-equatorial MS waves of a few hundred pT can act as an important candidate to cause the pitch angle scattering and momentum diffusion of radiation belt electrons at pitch angles $< \sim 75^\circ$ on timescales of a day and to produce electron butterfly distributions at energies of ~ 100 keV to > 1 MeV within an hour.

2. Analysis of the 8 May 2014 Event of Off-Equatorial MS Waves

2.1. Event Overview

The first off-equatorial MS event of our interest was observed on 8 May 2014 by the Electric Field and Waves Instrument (EFW) (Wygant et al., 2013) and the Electric and Magnetic Field Instrument Suite and Integrated Science (EMFISIS) (Kletzing et al., 2013) on board Van Allen Probes (Mauk et al., 2013). During this time interval, since both probes crossed along almost the same trajectory and measured the MS emissions with a time difference < 1 h, here we only analyze the waves observed by Van Allen Probe A.

Figure 1a shows the background plasma density inferred from the measurements of upper hybrid resonance frequency (f_{uhz}), and Figures 1b-1f respectively illustrate the spectrograms of the magnetic (B_{psd}) and electric (E_{psd}) field power spectral density, the ellipticity, the wave normal angle, and the integrated magnetic field amplitude (B_w) of the MS waves. Clearly, a class of intense electromagnetic waves occurred with harmonic structures located between the proton gyrofrequency (f_{cp} , the blue solid curves) and the lower hybrid resonance frequency (f_{lhr} , the white solid curves) during the time period from 10:00 UT to $\sim 12:40$ UT. Figures 1d and 1e show that these electromagnetic waves were linearly polarized and propagating nearly perpendicularly to the ambient magnetic field at the wave normal angles predominantly above 80° , indicating that they are typical MS waves. During this time period, the plasma density increased from less than 10 cm^{-3} to $\sim 1,000 \text{ cm}^{-3}$, suggesting that these MS emissions occurred both inside and outside the plasmasphere. The variation of integrated magnetic field (B_w) amplitude of the MS waves is also mapped along the inbound trajectory of the spacecraft during the time from 09:00 UT to 13:00 UT, as illustrated in Figure 1g. The intense waves with $B_w > 100$ pT from 10:51 UT to 12:21 UT are marked with red arrows in Figure 1g, when the spacecraft moved from the magnetic latitude of 8.1° at $L = 4.2$ (t1), through the highest latitude of 9.2° at $L = 3.5$ at 11:45 UT (also marked with a red arrow, t2), to the lower latitude of 7.5° at $L = 2.3$ (t3). Figure 1h shows the time series of the geomagnetic indices (Dst and AE) and IMF B_z with a 5 min resolution (ftp://spdf.gsfc.nasa.gov/pub/data/omni/high_res_omni) from 12:00 UT on 7 May to 00:00 UT on 9 May 2014, in which the time interval of the off-equatorial MS waves is shaded. This strong off-equatorial MS wave event occurred during the recovery phase of a moderate geomagnetic storm with $(\text{Dst})_{\text{min}} \sim -60$ nT, moderate substorm activity, and a sudden southward turning of IMF B_z . An analysis of the wave spectral intensity at $L = 3.8 \pm 0.1$ (corresponding to the shaded region in Figures 1a-1f) is shown in Figure 1i. The gray curves present the observed wave spectral intensities during the shaded time interval, and the bold black curve represents their average profile. Evidently, the peak wave spectral intensity approached $\sim 0.8 \text{ nT}^2/\text{Hz}$ at ~ 30 Hz and the secondary peak reached $2 \times 10^{-2} \text{ nT}^2/\text{Hz}$ at ~ 60 – 90 Hz. The average profile manifests strong off-equatorial MS waves with $B_w = 590$ pT at the geomagnetic latitude $\sim 9.2^\circ$.

2.2. Electron Diffusion by the Wave

In order to investigate quantitatively the resonant interactions between the off-equatorial MS waves and radiation belt electrons, we perform test particle simulations to compute the bounce-averaged pitch angle ($\langle D_{aa} \rangle$), momentum ($\langle D_{pp} \rangle$), and mixed pitch angle-momentum ($\langle |D_{ap}| \rangle$) diffusion coefficients for radiation belt electrons from 10 keV to 4 MeV, the results of which are plotted in Figures 2a–2c. It is worthwhile to

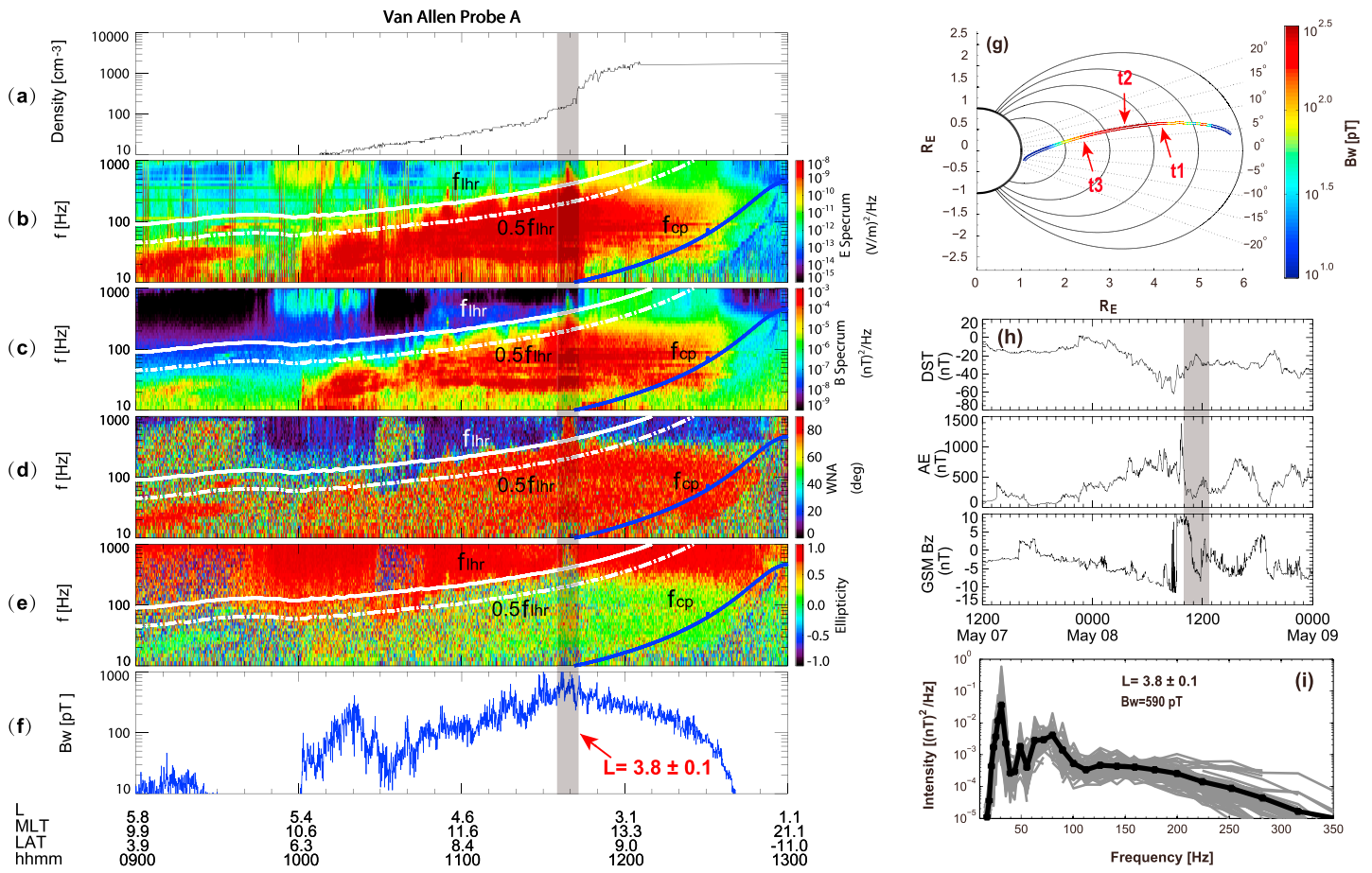


Figure 1. An overview of the off-equatorial MS event on 8 May 2014 observed by Van Allen Probe A from 09:00 to 13:00 UT: (a) the plasma density; the power spectral density of (b) the electric field (E_{psd}) and (c) the magnetic field (B_{psd}); (d) the wave normal angle and (e) the ellipticity. The white solid and dotted curves represent the lower hybrid resonant frequency (f_{LHR}) and half of lower hybrid resonant frequency ($0.5f_{\text{LHR}}$), respectively; the proton cyclotron frequency (f_{cp}) is denoted by the blue solid curve. (f) The integrated magnetic field amplitude of the off-equatorial MS waves (B_w); the interval of $L = 3.8 \pm 0.1$ is shaded in Figures 1a–1f; (g) the trajectory of Van Allen Probe A and the corresponding B_w with the red arrows showing the portion of our interest (t1: 10:51 UT, $L = 4.2$, Lat = 8.1°; t2: 11:45 UT, $L = 3.5$, Lat = 9.2°; t3: 12:21 UT, $L = 2.3$, Lat = 7.5°); (h) the time series of Dst, AE, and IMF B_z during the period of 12 UT, 7 May to 00 UT, 9 May 2014, in which the interval of the wave event is shaded; (i) scatterplots of the magnetic field spectral intensities of the off-equatorial MS waves (multiple gray curves) at $L = 3.8 \pm 0.1$, and the average profile (black solid curve).

note that the wave frequency spectral model is constructed exactly following the average spectral intensity profile (the bold thick curve) in Figure 1i. Following previous studies (e.g., Fu et al., 2016; Li, Ni, et al., 2016), we set the wave normal angle $\theta = 89.5^\circ$ instead of a Gaussian distribution in $\tan(\theta)$ as in Horne et al. (2007). To focus on the scattering effect of off-equatorial MS waves, we further assume that the observed MS emissions are confined within the magnetic latitudes of 7.5°–9.2° (as shown in Figure 1g) and latitudinally constant in the dipole geomagnetic field configuration. The ambient plasma density takes the average value of 130 cm^{-3} over $L = 3.8 \pm 0.1$ and is also assumed latitudinally constant. In addition, since we consider that the MS waves are absent below the magnetic latitude of 7.5°, the upper limit of the equatorial pitch angle that can undergo resonance with the off-equatorial emissions in the dipolar geometry is approximately 74.3°, justifying the blank region of diffusion rates above it shown in Figures 2a–2c. Generally, there is a broad region of both pitch angle and momentum diffusion coefficients at the rates of $\sim 10^{-5} \text{ s}^{-1}$, which is centered between equatorial pitch angles of ~40° to 70° and electron energies of approximately hundreds of keV to 2 MeV, mainly due to the Landau resonance between the waves and electrons (e.g., Horne et al., 2007; Li et al., 2014; Li, Ni, et al., 2016; Li, Bortnik, et al., 2016). As a consequence, the observed intense off-equatorial MS waves can transport a large population of radiation belt electrons at intermediate-to-high pitch angles on timescales of a day. Since pitch angle scattering rates are extremely small at low pitch angles near the loss cone, the off-equatorial MS waves have little effect on the scattering loss processes of

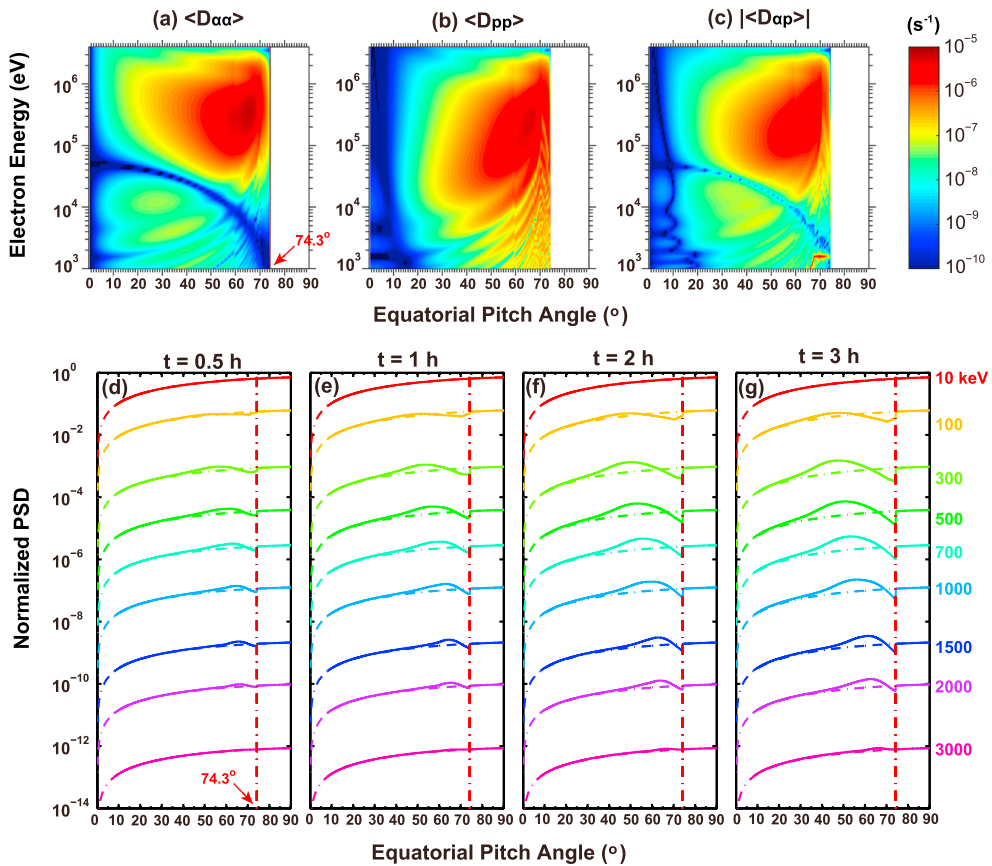


Figure 2. Corresponding to Figure 1, (a–c) test particle-simulated bounce-averaged pitch angle diffusion coefficients ($\langle D_{\alpha\alpha} \rangle$), momentum diffusion coefficients ($\langle D_{pp} \rangle$), and mixed pitch angle-momentum diffusion coefficients ($\langle |D_{ap}| \rangle$) as a function of equatorial pitch angle and electron kinetic energy, due to the impact of the off-equatorial MS waves at $L = 3.83.8 \pm 0.1$ on 8 May 2014; (d–g) simulated 3 h temporal evolution of normalized electron phase space density at color-coded energies. The initial electron PSD distributions are shown as dash-dotted curves and assumed to follow a kappa distribution. The vertical dash-dotted lines denote the upper limit of equatorial pitch angle that can resonate with the waves, that is, 74.3°.

radiation belt electrons. In contrast, the strong momentum diffusion at higher pitch angles suggests that the waves be a viable candidate for energetic electron acceleration.

Using the bounce-averaged electron scattering coefficients ($\langle D_{\alpha\alpha} \rangle$, $\langle D_{pp} \rangle$, and $\langle |D_{ap}| \rangle$) obtained through test particle simulations, we simulate the 3 h evolution of radiation belt electron phase space density (PSD) f by numerically solving the 2-D Fokker-Planck equation. For the boundary condition in the energy space, we assume that the electron PSDs are constant at $E_k = 1$ keV and 10 MeV with $f = 0$ at 10 MeV, and we take an empty loss cone and $\frac{\partial f}{\partial \alpha_{eq}}|_{\alpha_{eq}=90^\circ} = 0$ at the upper limit of equatorial pitch angle for the boundary condition in the equatorial pitch angle space, following previous studies (e.g., Li, Ni, et al., 2016; Li, Bortnik, et al., 2016; Ni et al., 2017). For simplicity, the initial radiation belt electron PSD distribution is modeled using a kappa distribution with the kappa index $\kappa = 6$ and effective thermal parameter $\theta^2 = 0.15$, following the study of Ma et al. (2016).

The temporal evolution of electron PSD for nine electron energies between 10 keV and 3 MeV is color coded in Figures 2d–2g for the indicated four time instances of resonant wave-particle interactions (i.e., 0.5 h, 1 h, 2 h, and 3 h). Note that in each panel the dotted curves represent the initial distribution of electron PSD. The vertical dotted line in each panel represents the upper limit of equatorial pitch angle in resonance, that is, 74.3°, corresponding to the boundary of diffusion rates in Figures 2a–2c. Evidently, the observed off-equatorial MS waves can efficiently diffuse 100 keV to 2 MeV electrons at pitch angles $\sim 70^\circ$ to $\sim 40^\circ$ – 60° pitch angles, thus facilitating the formation of energetic electron butterfly distributions within an hour (Figure 2e). As shown in Figures 2e–2g, the transport process continues with time and the butterfly distribution evolves more pronouncedly, regardless of electron energy (except for 10 keV due to the fixed boundary condition).

The most marked evolution of electron PSD occurs for 300 keV to 1 MeV. As electron energy further increases, the electron PSD grows much slower, while its peak moves toward higher equatorial pitch angles.

Previous studies (e.g., Bortnik & Thorne, 2010; Horne et al., 2007; Li, Ni, et al., 2016; Li, Bortnik, et al., 2016) reported that equatorial MS waves can accelerate energetic electrons preferentially at equatorial pitch angles 60°–80°. Zhao et al. (2014) also showed the persistent occurrence of electron butterfly distributions in the hundreds of keV range, for which they suggested that MS waves may play a role for the formation of such features in the inner zone and slot region. Our results, for example, Figure 2g, indicate that off-equatorial MS waves can cause electron PSD increase distinctly at lower pitch angles with the peak ~40°, especially for electrons at lower energies (100–300 keV), mainly due to the confinement of MS waves to a very narrow, off-equatorial latitudinal region. This result is consistent with the study of Ni et al. (2016) statistically showing that the pronounced butterfly distributions of ultrarelativistic electrons ($>\sim 1$ MeV) are mainly observed on the nightside at larger L shells ($L > 5$) with the averaged flux peak at pitch angles $\sim 50^\circ$ – 55° . Therefore, it is suggestive that strong off-equatorial MS wave-induced electron diffusion contribute to the formation of pronounced butterfly distribution of outer zone energetic electrons.

3. Analysis of the 9 January 2014 Event of Off-Equatorial MS Waves

3.1. Event Overview

On 9 January 2014 Van Allen Probe A captured another off-equatorial MS wave event, the overview of which is shown in Figure 3. Apparently, the MS emissions primarily occurred within a narrow frequency range of ~ 20 Hz to 30 Hz during the time interval of 06:36–07:41 UT (Figures 3b–3e), before which the spacecraft flew across a typical plasmapause into the plasmatrough with the electron density quickly decreasing from $>1,000 \text{ cm}^{-3}$ to $<\sim 100 \text{ cm}^{-3}$ (Figure 3a). Compared to the 8 May 2014 event, these MS waves were present at much higher geomagnetic latitudes of -17.5° to -15.7° (t1 to t2), while their wave amplitudes were much smaller with the peak value near 100 pT (Figures 3f and 3g). The time series of the Dst, AE, and IMF B_z indicate that this weaker but higher latitude MS wave event was observed during the recovery phase of a moderate storm and a southward IMF B_z interval. On the basis of the waves measured at $L = 5.4 \pm 0.1$ (the shaded region in Figures 3a–3f and 3h), we display the analysis of the wave spectral intensities in Figure 3i, showing that the average wave spectral intensity follows a Gaussian function-type distribution. Using the least squares Gaussian fit (e.g., Ni et al., 2015), we obtain the model of this MS wave event (the red curve in Figure 3i) adopted for following evaluations. The average off-equatorial MS wave amplitude is about 81 pT, with the center frequency at $f_m = 25.2$ Hz, and the wave bandwidth $\delta f = 1.9$ Hz.

3.2. Electron Diffusion by the Wave

Following the same procedure of analyzing the 8 May 2014 event, we compute the bounce-averaged diffusion coefficients via test particle simulations and model the 3 h temporal evolution of radiation belt electron PSD via 2-D diffusion simulations for the 9 January 2014 event, the results of which are displayed in Figures 4a–4g. The Gaussian wave model obtained from Figure 3i is assumed to be confined within the magnetic latitudes of $(-17.5^\circ$ – $15.7^\circ)$ and latitudinally constant. The averaged plasma density is set as 29 cm^{-3} at $L = 5.4 \pm 0.1$ and also assumed latitudinally constant. As a consequence of the dipole field geometry, the maximal equatorial pitch angle of radiation belt electrons that can resonate with these off-equatorial MS emissions is approximately 58.1° , as indicated in each panel of Figure 4.

Compared to the first event, these MS waves at higher latitudes tend to produce the strongest electron diffusion rates toward lower equatorial pitch angles and lower kinetic energies. Specifically, for ~ 10 keV to 1 MeV electrons, the diffusion rates are dominant at equatorial pitch angles of $\sim 45^\circ$ – 55° , mostly due to the Landau resonance. At higher energies, the transit time scattering effect may become dominant. However, it is worthwhile to note that the MS wave-induced scattering rates only peak at the level of 10^{-6} s^{-1} , inferring that it takes about 10 days or more for the observed MS waves to diffuse energetic electrons in the pitch angle and/or momentum space. Overall, the scattering effect of the MS waves in this event is weak. The 3 h evolution of electron PSD from 10 keV to 3 MeV shows very small variations (Figures 4d–4g), in which a slight peak in electron PSD occurs for 300–700 keV electrons after at least 1 h interactions with the off-equatorial emissions. It is worthwhile to note that while the computed MS wave scattering effect is weak, the adoption of a 3 h simulation is reasonably consistent with the wave observations by the two Van Allen Probes.

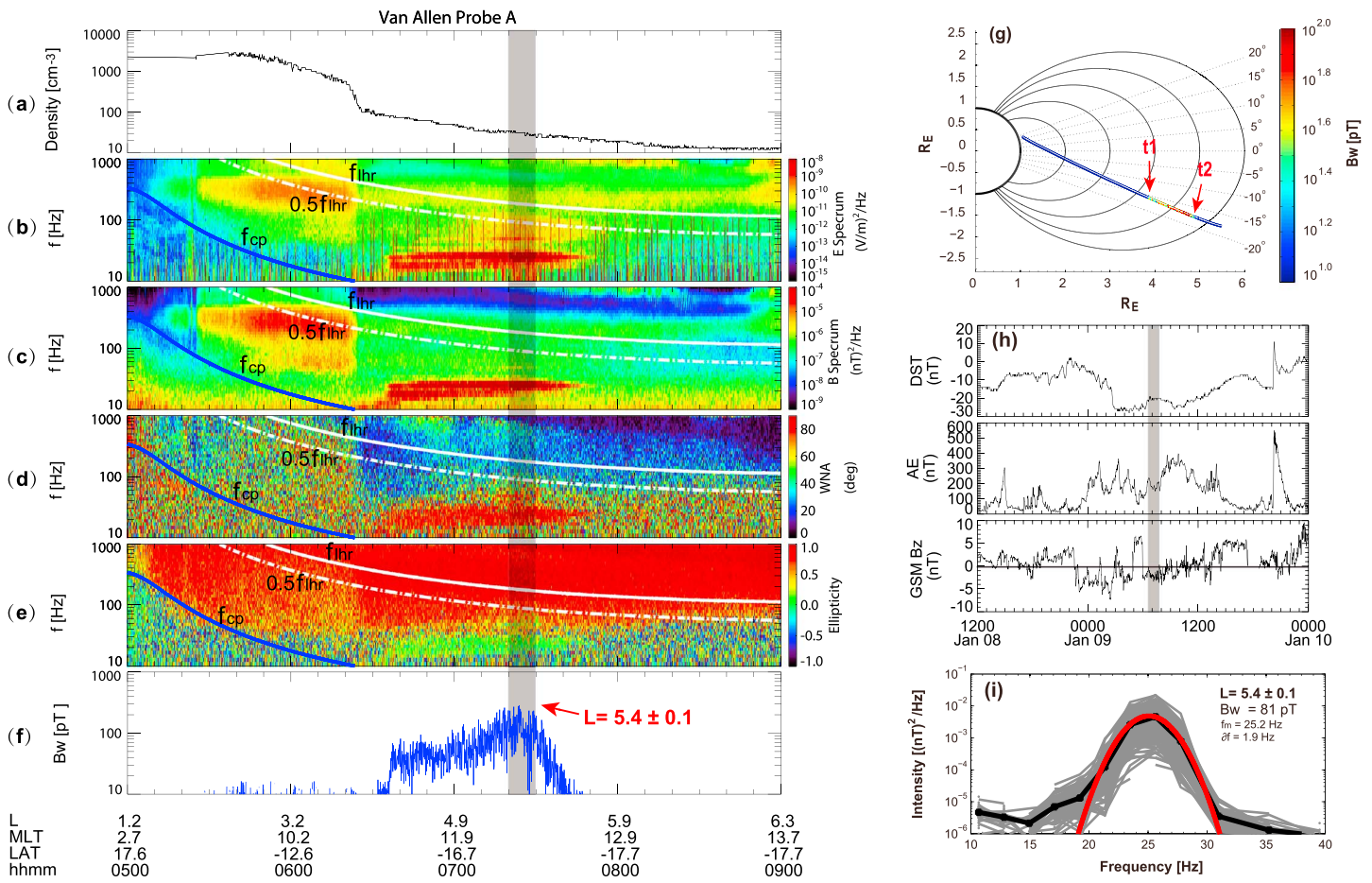


Figure 3. Same as in Figure 1, except for the off-equatorial MS wave event observed by Van Allen Probe A at 05–09 UT on 9 January 2014. In Figure 3g, the label “t1” denotes the time and location at 06:36 UT, $L = 4.3$, and Lat = -15.7° , and t2 at 07:41 UT, $L = 5.6$, and Lat = -17.5° .

Apparently, compared to the 8 May 2014 wave event, the 9 January 2014 wave event cannot efficiently redistribute the pitch angle profile and energy spectrum of radiation belt electrons within a few hours. Interestingly, Li, Ni, et al. (2016) reported that energetic radiation belt electrons at intermediate pitch angles can be quickly accelerated by equatorial MS waves to facilitate the formation of butterfly distributions within a couple of hours or less. However, Ma et al. (2016) showed that no obvious butterfly distributions of normalized electron PSD can be registered within 4 h interactions with equatorial MS waves. It is worthwhile to point out that, corresponding to these different results, different wave amplitudes of MS emissions were adopted. The average wave amplitude was 590 pT for the 8 May 2014 wave event and was 240 pT for the analysis of Li, Ni, et al. (2016), while it became smaller to be ~ 100 pT for the 9 January 2014 wave event and ~ 60 pT on the dayside and ~ 25 pT on the nightside for the analysis of Ma et al. (2016). Therefore, it is strongly suggested that the intensity of MS waves, either equatorial or off-equatorial, should play as a key or even dominant factor in the wave-induced electron scattering effect, which, however, is outside the scope of the present study and requires detailed parametric investigation.

4. Discussions and Conclusions

While the features of equatorial MS waves and their diffusion effects on radiation belt electrons have been largely investigated, the present study has looked into the high-quality data sets of magnetospheric waves measured by Van Allen Probes and reported two interesting off-equatorial MS events, that is, the 8 May 2014 event that occurred at the geomagnetic latitudes of 7.5° – 9.2° both inside and outside the plasmasphere with the wave amplitude up to 590 pT, and the 9 January 2014 event that occurred at the latitudes of $-(15.7^\circ$ – $17.5^\circ)$ outside the plasmasphere with a smaller amplitude about 81 pT.

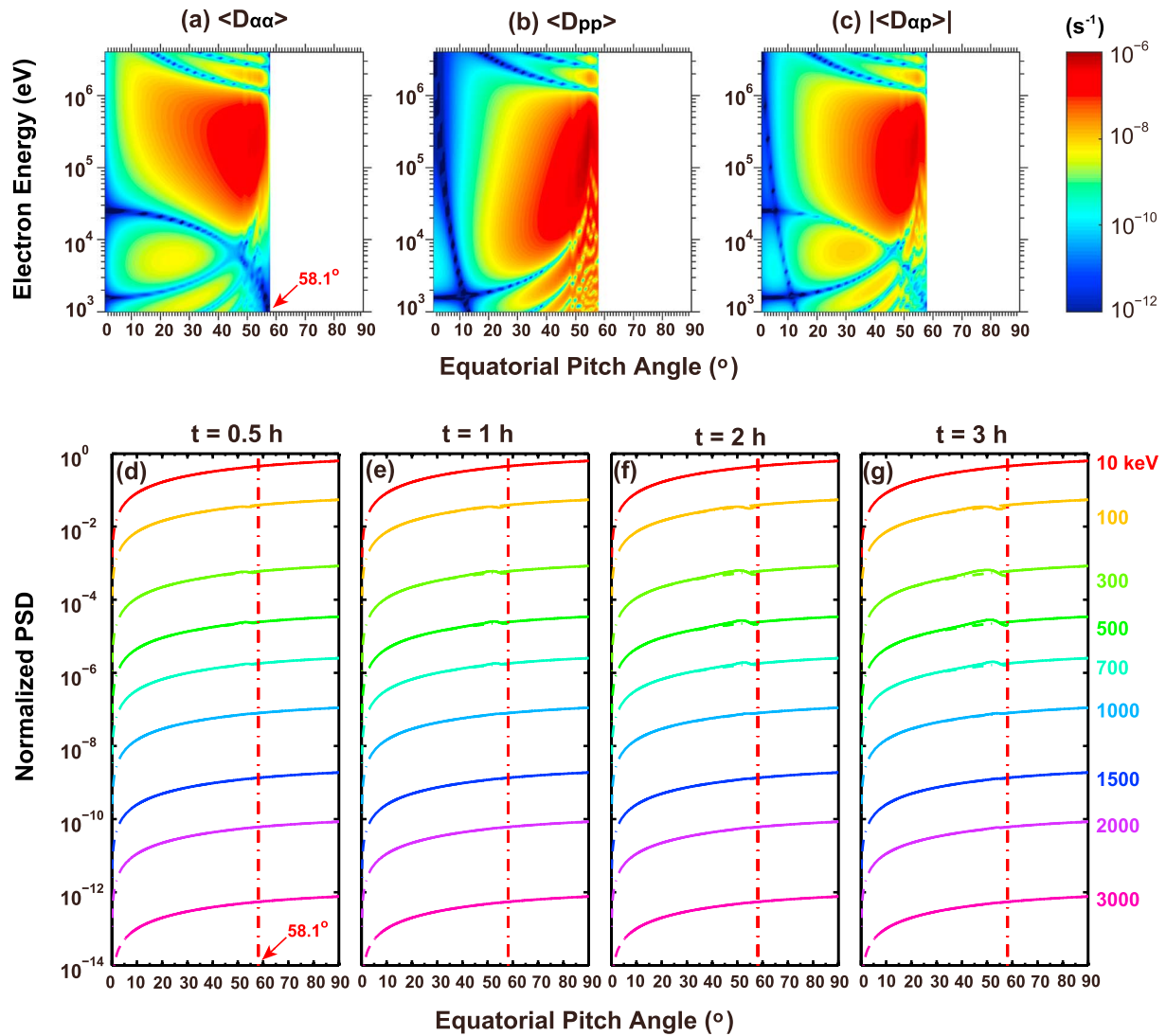


Figure 4. Same as in Figure 2, except for the 9 January 2014 MS wave event at $L = 5.4 \pm 0.1$. The vertical dash-dotted lines denote the upper limit of equatorial pitch angle that can resonate with the waves, that is, 58.1° .

We have performed detailed test particle simulations to compute the electron resonant scattering rates by the off-equatorial MS waves to find that they can cause the pitch angle scattering and momentum diffusion of radiation belt electrons with equatorial pitch angles $< \sim 75^\circ$ on timescales of a day. Subsequent two-dimensional Fokker-Planck diffusion simulations have also indicated that the strong off-equatorial MS waves are capable of efficiently transporting high pitch angle electrons to lower pitch angles to facilitate the formation of electron butterfly distributions for a broad energy range from ~ 100 keV to > 1 MeV within an hour.

While this study focuses on the off-equatorial MS waves and the spacecraft location of the considered periods were not ideal to observe the equatorial emissions, it is quite probable that the MS waves occur at the equatorial region as well. In a similar manner, we have performed numerical simulations to quantify the electron scattering effects by the lower latitude and equatorial MS emissions. The results (see supporting information) indicate that the diffusion rates driven by equatorial MS waves can extend to equatorial pitch angles very close to 90° , for which the gaps shown in Figures 2 and 4 disappear, because the electrons at all equatorial pitch angles can interact with the MS waves when they are present at the equatorial region. It is also seen that, given wave amplitude, the MS emissions at lower latitudes tend to produce stronger rates of electron pitch angle diffusion and more pronounced features of electron butterfly pitch angle distribution on a shorter timescale.

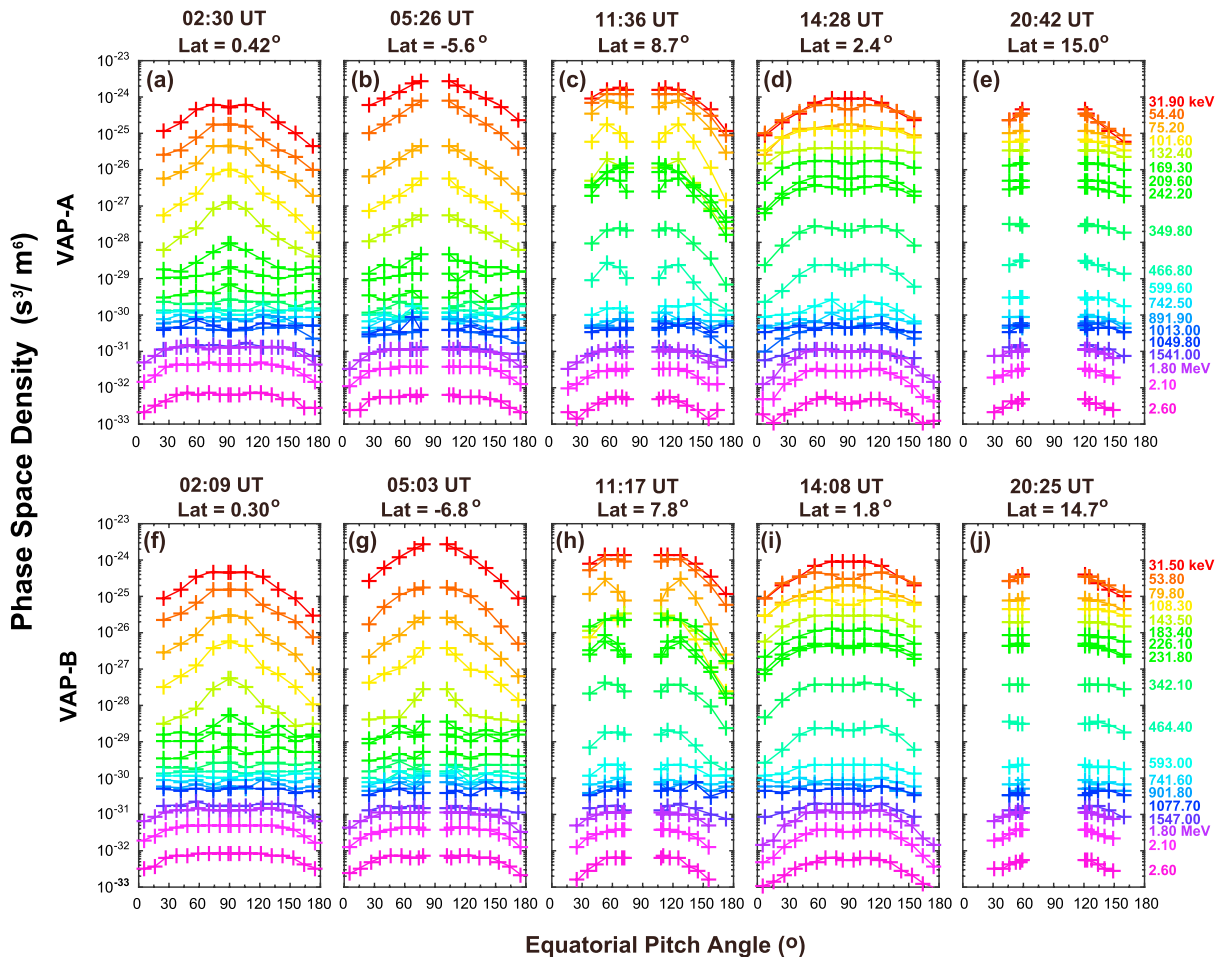


Figure 5. Van Allen Probes (A and B) measured electron phase space density profiles at $L \sim 3.8$ as a function of equatorial pitch angle (mapped for local pitch angle) for a number of color-coded electron energies from ~ 30 keV to 2.6 MeV at the indicated time stamps on 8 May 2014.

In order to further check the electron scattering effects of off-equatorial MS waves and their contribution to the formation of electron butterfly distribution, we also compare the Van Allen Probes-measured electron distributions with the simulated ones for the 8 May 2014 event, the results of which are shown in Figure 5. Note that we have converted the local pitch angles to equatorial pitch angles on the basis of a dipolar field geometry. It is shown that while no butterfly distributions were present before the strong MS wave activity (i.e., 02:30 UT and 05:26 UT), they formed at energies of ~ 75 – 600 keV with the occurrence of strong off-equatorial MS waves (i.e., 11:36 UT) but decayed quickly and become almost invisible after ~ 3 h (i.e., 14:28 UT and 20:42 UT). Comparisons between these observations with the model results (i.e., Figures 2d–2g) indicate that scattering by the off-equatorial MS waves tends to reasonably reproduce the butterfly distribution feature of ~ 100 – 500 keV electrons but obviously overestimate the butterfly occurrence at higher energies around 11:36 UT. According to our above detailed analysis, scattering by off-equatorial MS waves can contribute largely to the formation of butterfly distributions within a couple of hours during the period of intense wave activity. Since both satellites did not capture the MS waves in the following orbiting trajectories, the off-equatorial MS waves lasted very probably just for a few hours (< 3 h), which suggests that the electron butterfly distributions can be unstable and should not persist during the absence of MS waves. In addition, there can be the possibility of other wave-particle interaction mechanisms in the outer radiation belt, including scattering by hiss, EMIC waves, and chorus (e.g., Ni et al., 2013, 2018; Thorne, 2010), that may inhibit the butterfly distribution formation. Therefore, scattering by the off-equatorial MS waves alone cannot fully explain the observed radiation belt electron variations during the 8 May 2014 event for which some other wave-particle interaction mechanisms need to be reasonably incorporated.

Overall, our study clearly demonstrates that the presence of off-equatorial MS waves, in addition to equatorial MS waves, can contribute importantly to the dynamical variations of radiation belt electron fluxes and their pitch angle distribution, which, however, requires further quantitative investigation in following studies.

Acknowledgments

The work was supported by the NSFC grants 41674163, 41474141, and 41204120 and the Hubei Province Natural Science Excellent Youth Foundation (2016CFA044). We thank the Van Allen Probes EMFISIS Science Team including Craig Klezting, William Kurth, and George Hospodarsky for providing the data. The EMFISIS data are obtained from <https://emfisis.physics.uiowa.edu/data/index>. The data of geomagnetic indices are available from the NASA OmniWeb (<http://cdaweb.gsfc.nasa.gov>). Comparisons of the effects of off-equatorial MS waves with those of lower latitude and equatorial MS waves and the Van Allen Probes measured electron distributions for the 8 May 2014 event are shown in the supporting information.

References

- Balikhin, M. A., Shprits, Y. Y., Walker, S. N., Chen, L., Cornilleau-Wehrlin, N., Dandouras, I., et al. (2015). Observations of discrete harmonics emerging from equatorial noise. *Nature Communications*, 6(1). <https://doi.org/10.1038/ncomms8703>
- Boardsen, S. A., Hospodarsky, G. B., Kletzing, C. A., Pfaff, R. F., Kurth, W. S., Wygant, J. R., & MacDonald, E. A. (2014). Van Allen Probe observations of periodic rising frequencies of the fast magnetosonic mode. *Geophysical Research Letters*, 41, 8161–8168. <https://doi.org/10.1002/2014GL062020>
- Bortnik, J., & Thorne, R. M. (2010). Transit time scattering of energetic electrons due to equatorially confined magnetosonic waves. *Journal of Geophysical Research*, 115, A07213. <https://doi.org/10.1029/2010JA015283>
- Chen, L., & Thorne, R. M. (2012). Perpendicular propagation of magnetosonic waves. *Geophysical Research Letters*, 39, L14102. <https://doi.org/10.1029/2012GL052485>
- Chen, L., Thorne, R. M., Jordanova, V. K., Thomsen, M. F., & Horne, R. B. (2011). Magnetosonic wave instability analysis for proton ring distributions observed by the LANL magnetospheric plasma analyzer. *Journal of Geophysical Research*, 116, A03223. <https://doi.org/10.1029/2010JA016068>
- Fu, H. S., Cao, J. B., Zhima, Z., Khotyaintsev, Y. V., Angelopoulos, V., Santolik, O., et al. (2014). First observation of rising-tone magnetosonic waves. *Geophysical Research Letters*, 41, 7419–7426. <https://doi.org/10.1002/2014GL061867>
- Fu, S., Ni, B., Li, J., Zhou, C., Gu, X., Huang, S., et al. (2016). Interactions between magnetosonic waves and ring current protons: Gyroaveraged test particle simulations. *Journal of Geophysical Research: Space Physics*, 121, 8537–8553. <https://doi.org/10.1002/2016JA023117>
- Horne, R. B., Thorne, R. M., Glauer, S. A., Meredith, N. P., Pokhotelov, D., & Santolik, O. (2007). Electron acceleration in the van Allen radiation belts by fast magnetosonic waves. *Geophysical Research Letters*, 34, L17107. <https://doi.org/10.1029/2007GL030267>
- Kletzing, C. A., Kurth, W. S., Acuna, M., MacDowall, R. J., Torbert, R. B., Averkamp, T., et al. (2013). The Electric and Magnetic Field Instrument Suite and Integrated Science (EMFISIS) on RBSP. *Space Science Reviews*, 179(1–4), 127–181. <https://doi.org/10.1007/s11214-013-9993-6>
- Li, J., Bortnik, J., Li, W., Ma, Q., Thorne, R. M., Kletzing, C. A., et al. (2017). “Zipper-like” periodic magnetosonic waves: Van Allen Probes, THEMIS, and magnetospheric multiscale observations. *Journal of Geophysical Research: Space Physics*, 122, 1600–1610. <https://doi.org/10.1002/2016JA023536>
- Li, J., Bortnik, J., Thorne, R. M., Li, W., Ma, Q., Baker, D. N., et al. (2016). Ultrarelativistic electron butterfly distributions created by parallel acceleration due to magnetosonic waves. *Journal of Geophysical Research: Space Physics*, 121, 3212–3222. <https://doi.org/10.1002/2016JA022370>
- Li, J., Ni, B., Ma, Q., Xie, L., Pu, Z., Fu, S., et al. (2016). Formation of energetic electron butterfly distributions by magnetosonic waves via Landau resonance. *Geophysical Research Letters*, 43, 3009–3016. <https://doi.org/10.1002/2016GL067853>
- Li, J., Ni, B., Xie, L., Pu, Z., Bortnik, J., Thorne, R. M., et al. (2014). Interactions between magnetosonic waves and radiation belt electrons: Comparisons of quasi-linear calculations with test particle simulations. *Geophysical Research Letters*, 41, 4828–4834. <https://doi.org/10.1002/2014GL060461>
- Ma, Q., Li, W., Thorne, R. M., & Angelopoulos, V. (2013). Global distribution of equatorial magnetosonic waves observed by THEMIS. *Geophysical Research Letters*, 40, 1895–1901. <https://doi.org/10.1002/grl.50434>
- Ma, Q., Li, W., Thorne, R. M., Bortnik, J., Kletzing, C. A., Kurth, W. S., & Hospodarsky, G. B. (2016). Electron scattering by magnetosonic waves in the inner magnetosphere. *Journal of Geophysical Research: Space Physics*, 121, 274–285. <https://doi.org/10.1002/2015JA021992>
- Mauk, B. H., Fox, N. J., Kanekal, S. G., Kessel, R. L., Sibeck, D. G., & Ukhorskiy, A. (2013). Science objectives and rationale for the Radiation Belt Storm Probes mission. *Space Science Reviews*, 1–15. <https://doi.org/10.1007/s11214-012-9908-y>
- Meredith, N. P., Horne, R. B., & Anderson, R. R. (2008). Survey of magnetosonic waves and proton ring distributions in the Earth’s inner magnetosphere. *Journal of Geophysical Research*, 113, A06213. <https://doi.org/10.1029/2007JA012975>
- Ni, B., Bortnik, J., Thorne, R. M., Ma, Q., & Chen, L. (2013). Resonant scattering and resultant pitch angle evolution of relativistic electrons by plasmaspheric hiss. *Journal of Geophysical Research: Space Physics*, 118, 7740–7751. <https://doi.org/10.1002/2013JA019260>
- Ni, B., Cao, X., Shprits, Y., Summers, D., Gu, X., Fu, S., & Lou, Y. (2018). Hot plasma effects on the cyclotron-resonant pitch-angle scattering rates of radiation belt electrons due to EMIC waves. *Geophysical Research Letters*, 45. <https://doi.org/10.1002/2017GLR076028>
- Ni, B., Cao, X., Zou, Z., Zhou, C., Gu, X., Bortnik, J., et al. (2015). Resonant scattering of outer zone relativistic electrons by multi-band EMIC waves and resultant electron loss timescales. *Journal of Geophysical Research: Space Physics*, 120, 7357–7373. <https://doi.org/10.1002/2015JA021466>
- Ni, B., Hua, M., Zhou, R., Yi, J., & Fu, S. (2017). Competition between outer zone electron scattering by plasmaspheric hiss and magnetosonic waves. *Geophysical Research Letters*, 44, 3465–3474. <https://doi.org/10.1002/2017GL072989>
- Ni, B., Zou, Z., Li, X., Bortnik, J., Xie, L., & Gu, X. (2016). Occurrence characteristics of outer zone relativistic electron butterfly distribution: A survey of Van Allen Probes REPT measurements. *Geophysical Research Letters*, 43, 5644–5652. <https://doi.org/10.1002/2016GL069350>
- Russell, C. T., Holzer, R. E., & Smith, E. J. (1970). OGO 3 observations of ELF noise in the magnetosphere: 2. The nature of the equatorial noise. *Journal of Geophysical Research*, 75(4), 755–768. <https://doi.org/10.1029/JA075i004p0075>
- Santolik, O., Pickett, J. S., Gurnett, D. A., Maksimovic, M., & Cornilleau-Wehrlin, N. (2002). Spatiotemporal variability and propagation of equatorial noise observed by Cluster. *Journal of Geophysical Research*, 107(A12), 1495. <https://doi.org/10.1029/2001JA009159>
- Thorne, R. M. (2010). Radiation belt dynamics: The importance of wave-particle interactions. *Geophysical Research Letters*, 37, L22107. <https://doi.org/10.1029/2010GL044990>
- Tsurutani, B. T., Falkowski, B. J., Pickett, J. S., Verkhoglyadova, O. P., Santolik, O., & Lakhina, G. S. (2014). Extremely intense ELF magnetosonic waves: A survey of polar observations. *Journal of Geophysical Research: Space Physics*, 119, 964–977. <https://doi.org/10.1002/2013JA019284>
- Wygant, J. R., Bonnell, J. W., Goetz, K., Ergun, R. E., Mozer, F. S., Bale, S. D., et al. (2013). The electric field and waves instruments on the Radiation Belt Storm Probes mission. *Space Science Reviews*, 179(1–4), 183–220. <https://doi.org/10.1007/s11214-013-0013-7>
- Xiao, F., Yang, C., Su, Z., Zhou, Q., He, Z., He, Y., et al. (2015). Wave-driven butterfly distribution of Van Allen belt relativistic electrons. *Nature Communications*, 6(1), 8590. <https://doi.org/10.1038/ncomms9590>
- Xiao, F., Zhou, Q., He, Y., Yang, C., Liu, S., Baker, D. N., et al. (2015). Penetration of magnetosonic waves into the plasmasphere observed by the Van Allen Probes. *Geophysical Research Letters*, 42, 7287–7294. <https://doi.org/10.1002/2015GL065745>
- Zhao, H., Li, X., Blake, J. B., Fennell, J. F., Claudepierre, S. G., Baker, D. N., et al. (2014). Peculiar pitch angle distribution of relativistic electrons in the inner radiation belt and slot region. *Geophysical Research Letters*, 41, 2250–2257. <https://doi.org/10.1002/2014GL059725>
- Zhima, Z., Chen, L., Fu, H., Cao, J., Horne, R. B., & Reeves, G. (2015). Observations of discrete magnetosonic waves off the magnetic equator. *Geophysical Research Letters*, 42, 9694–9701. <https://doi.org/10.1002/2015GL066255>